SUPPLEMENTARY MATERIALS

Chlorophyll-depleted wheat mutants are disturbed in photosynthetic electron flow regulation but can retain an acclimation ability to a fluctuating light regime

Lorenzo Ferroni, Marek Živčak, Oksana Sytar, Marek Kovár, Nobuyoshi Watanabe, Simonetta Pancaldi, Costanza Baldisserotto, Marián Brestič

Figure 1. Environmental parameters monitoring at the Slovak PlantScreen™ Phenotyping Unit.

Figure 2. Light intensity variation during Dual-PAM measuring routine for analysis of PSII and PSI parameters.

Figure 3. CO_2 fixation properties as emerging from gas exchange analyses.

Figure 4. Time course of parameters related to PSII activity as emerging from Dual-PAM analyses.

Figure 5. Time course of parameters related to PSI activity as emerging from Dual-PAM analyses.

Figure 6. Time course of parameters related to the generation and use of the trans-thylakoidal proton motive force.

Figure 7. Time course of parameters related to the dynamic regulation of photosynthesis.

Figure 8. Examples of thylakoid architectures in chloroplasts of *chlorina* mutants of wheat.

Figure 9. Time course of the energy distribution to PSII (*dII*) and of the electron flow to sinks alternative to photosynthesis (J_A/J_{PSII}).

Figure 10. Plots of measured photosynthesis-related parameters *vs* final aboveground biomass accumulated by *Triticum* plants.

Supplementary Figure 1

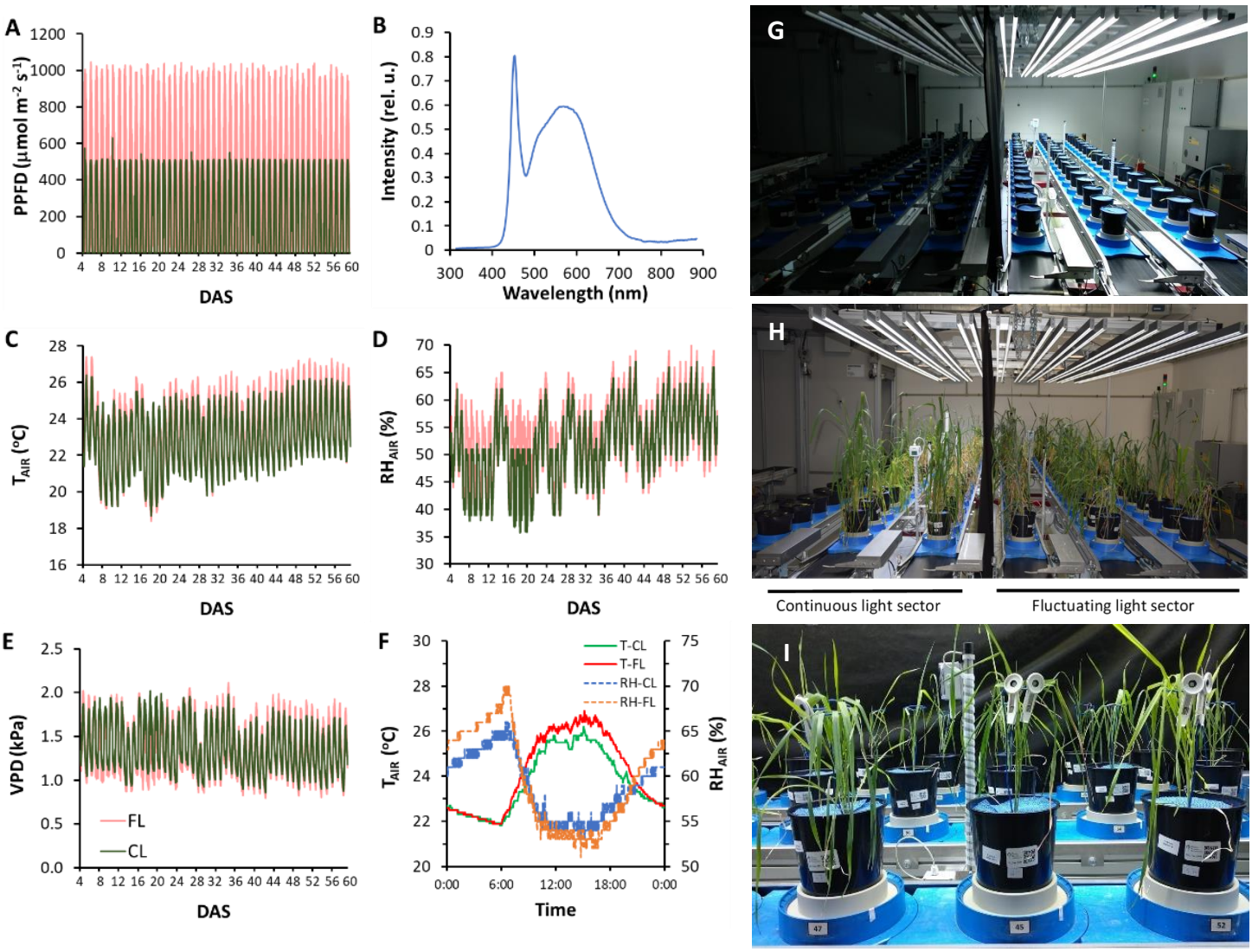

Environmental parameters monitoring at the Slovak PlantScreen™ Phenotyping Unit (SPPU).

(A) Photosynthetic photon flux density (PPFD) during the experimental period in the continuous light (CL, green) and fluctuating light (FL, pink) sectors (DAS, day after sowing). Note that the spikes of irradiance in FL sector reach 1000 µmol m^{-2} s^{-1}; diurnal PPFD variations are exemplified in Fig. 1 of the main text. (B) Spectral composition of the LED lights. (C) Air temperature (T), showing nearly overlapping values in the two sectors. (D) Relative humidity (RH) controlled so as to range between 40% and 65% in both sectors. (E) Vapour-pressure deficit (VPD) is overlapping between the two sectors thanks to the strict control of T and RH. (F) Example of a diurnal variation in T and RH in the two sectors. (G) Plant growth facility at SPPU at an early stage of the experiment during a simulated sunset – while light intensity is overall decreasing, in FL sector one of the last min-long light ramps enlightens the sector. (H) Plant growth facility at SPPU at a late stage of the experiment. (I) Details of some experimental plants, showing the bar codes on the pots for registration into the system.

Supplementary Figure 2

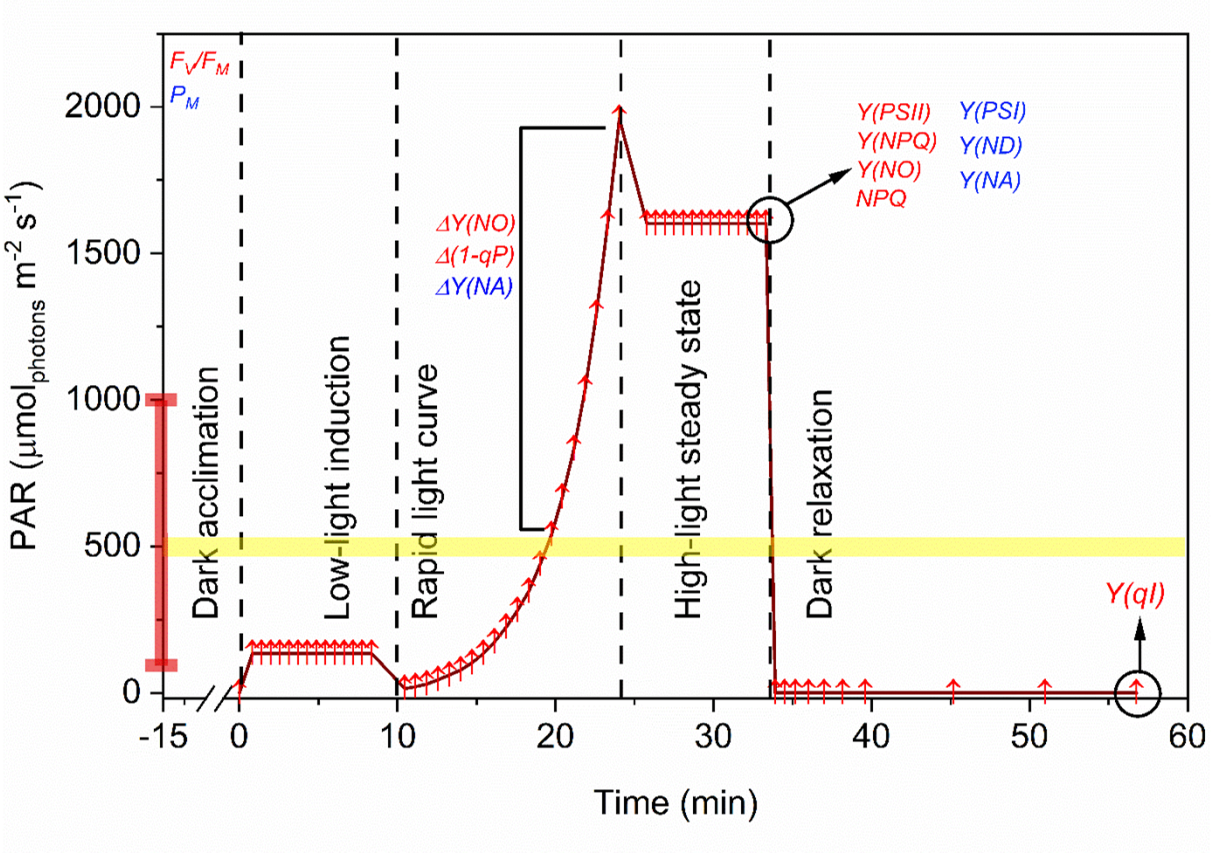

Light intensity variation during Dual-PAM measuring routine for analysis of PSII and PSI parameters, indicated with red and blue letters, respectively.

After the initial dark acclimation, the samples were exposed to a sequence of photosynthetically active radiation (PAR) at variable intensity. Arrows represent the time points at which a saturation pulse was applied. The yellow band shows the approximate value of irradiance in the CL sector in the middle of photoperiod. The red segment on the y axis approximates the range of irradiance fluctuations in the FL sector.

After determination of the dark-acclimated parameters, the leaf was allowed to reach a steady state at low actinic light to activate the photosynthetic process. Subsequently, a rapid light curve was triggered: the dynamic change of the indicated parameters was analysed comparing their values between the extremes comprised by the square bracket (539-1960 µmol photons m^{-2} s^{-1}).

In the following step, a 7-min long exposure to high light was performed to evaluate steady-state parameters. Finally, a relaxation period of 20 min in darkness was allowed to analyse the extent of PSII quantum yield recovery (and thus of photoinhibition).

Definition of parameters is reported in the main text.

Supplementary Figure 3

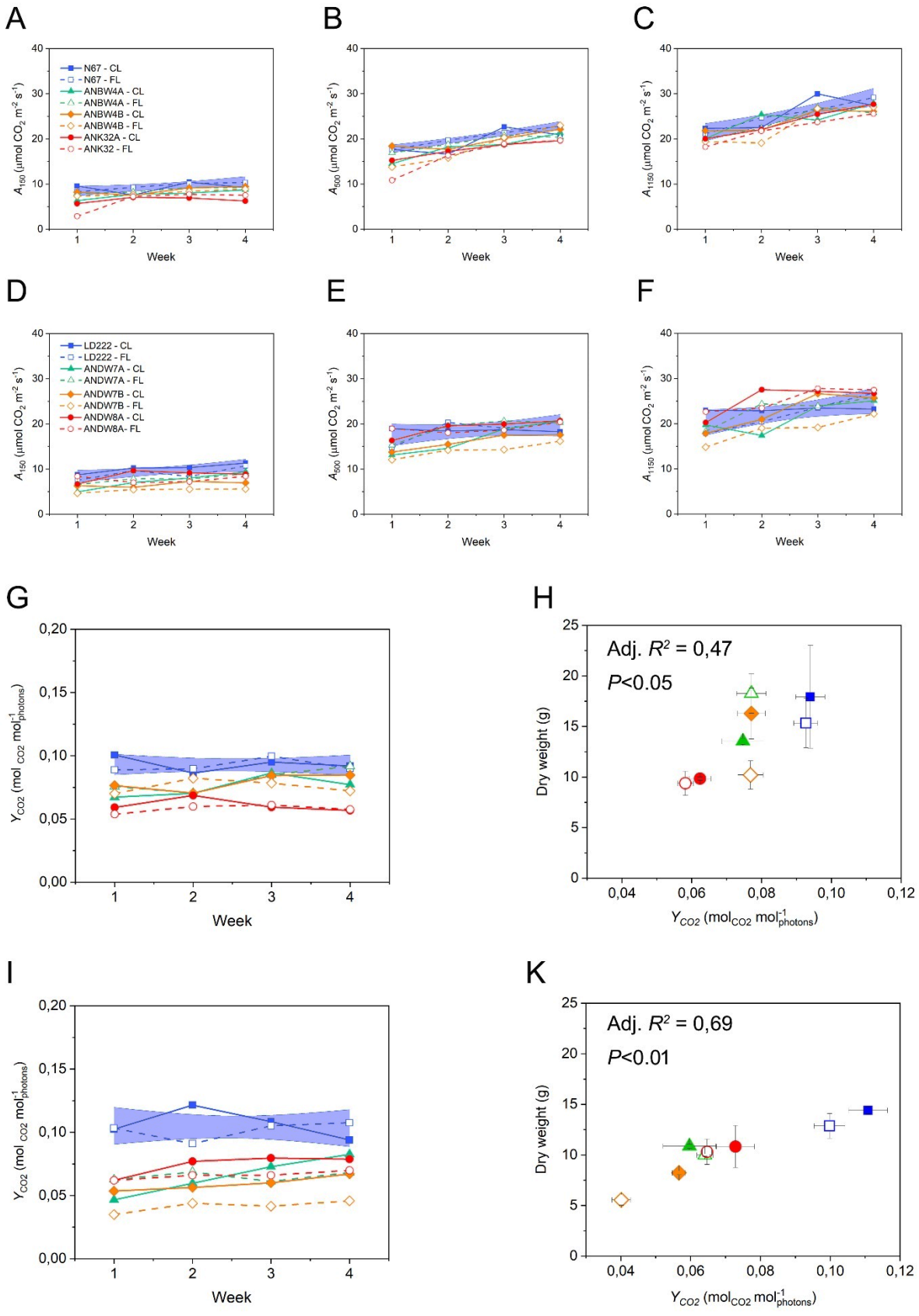

CO_2 fixation properties as emerging from gas exchange analyses of WT *Triticum aestivum* (bread wheat) and *T. durum* (durum wheat) and their *chlorina* mutants, cultivated in a continuous (CL) or fluctuating light regime (FL). Each time-course graph reports single parameters obtained during a 4-week long monitoring, 32 (week 1) to 55 DAS (week 4). For comparison of mutants, as background information in each graph the confidence bands at 95% probability are drawn after linear regression of all WT values.

(A-C) Time course of CO_2 assimilation *A* in bread wheat at irradiance values representative for low light condition (e.g. minimum irradiance under FL), average growth light and high light (e.g., an irradiance peak under FL).

(D-F) Time course of CO_2 assimilation *A* in durum wheat, at irradiance values representative for low light condition (e.g. minimum irradiance under FL), average growth light and high light (e.g., an irradiance peak under FL).

(G) Time course of CO_2 assimilation yield Y_{CO2} in bread wheat.

(H) Covariation of Y_{CO2} and final aboveground dry weight in bread wheat. Information about significance of correlation is reported in the graph.

(I) Time course of CO_2 assimilation yield Y_{CO2} in durum wheat.

(K) Covariation of Y_{CO2} and final aboveground dry weight in durum wheat. Information about significance of correlation is reported in the graph.

Supplementary Figure 4

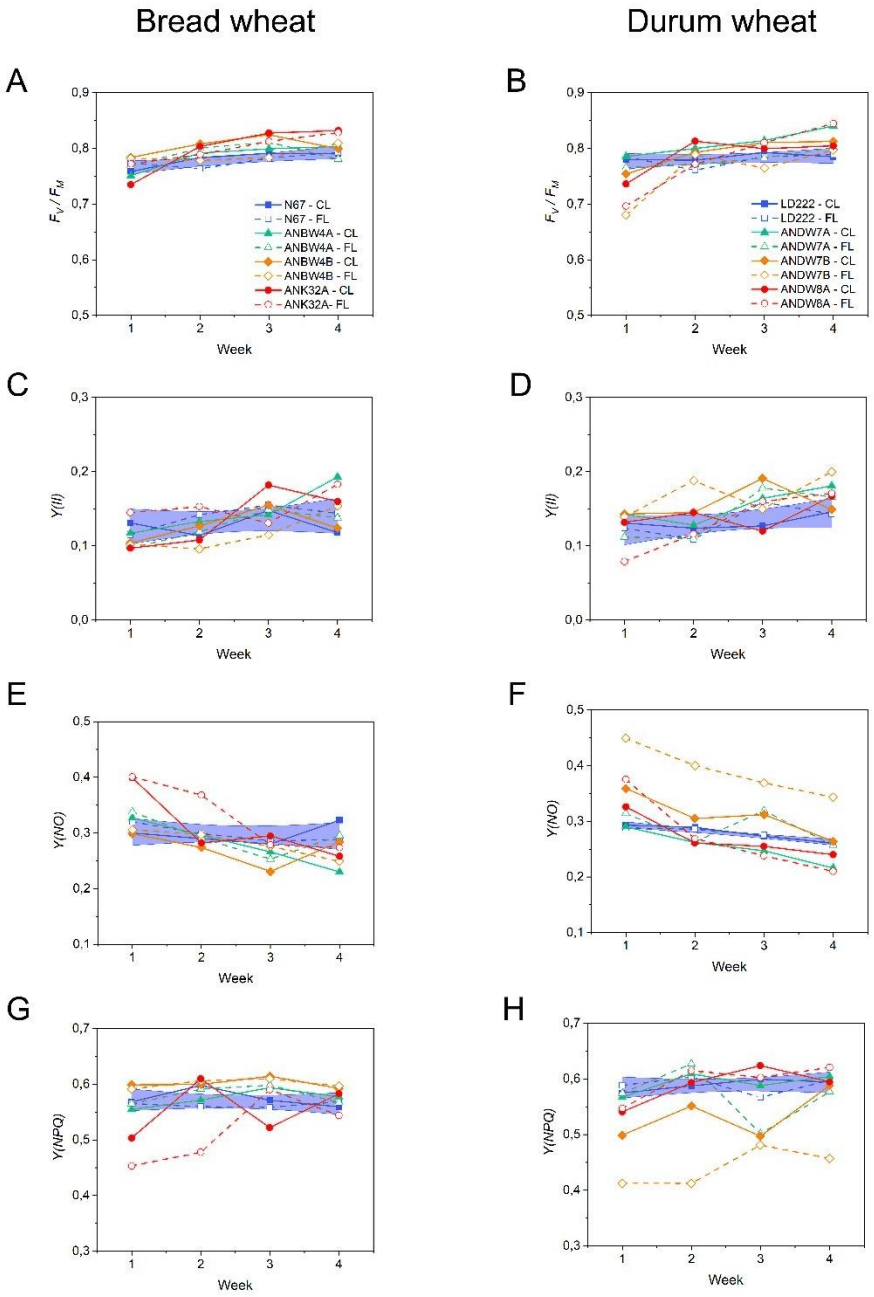

Time course of parameters related to PSII activity as emerging from Dual-PAM analyses of WT *Triticum aestivum* (bread wheat) and *T. durum* (durum wheat) and in their *chlorina* mutants, cultivated in a continuous (CL) or fluctuating light regime (FL). Maximum quantum yield of PSII photochemistry F_V/F_M was evaluated in the dark-acclimated state; actual quantum of PSII photochemistry *Y(PSII)*, of non-regulatory energy dissipation *Y(NO)*, and of regulatory energy dissipation *Y(NPQ)* were measured at the steady state in samples acclimated to high light for 7 min. Each graph reports single parameters obtained during a 4-week long monitoring, 32 to 55 DAS. For comparison of mutants, as background information in each graph the confidence bands at 95% probability are drawn after linear regression of all WT values.

Supplementary Figure 5

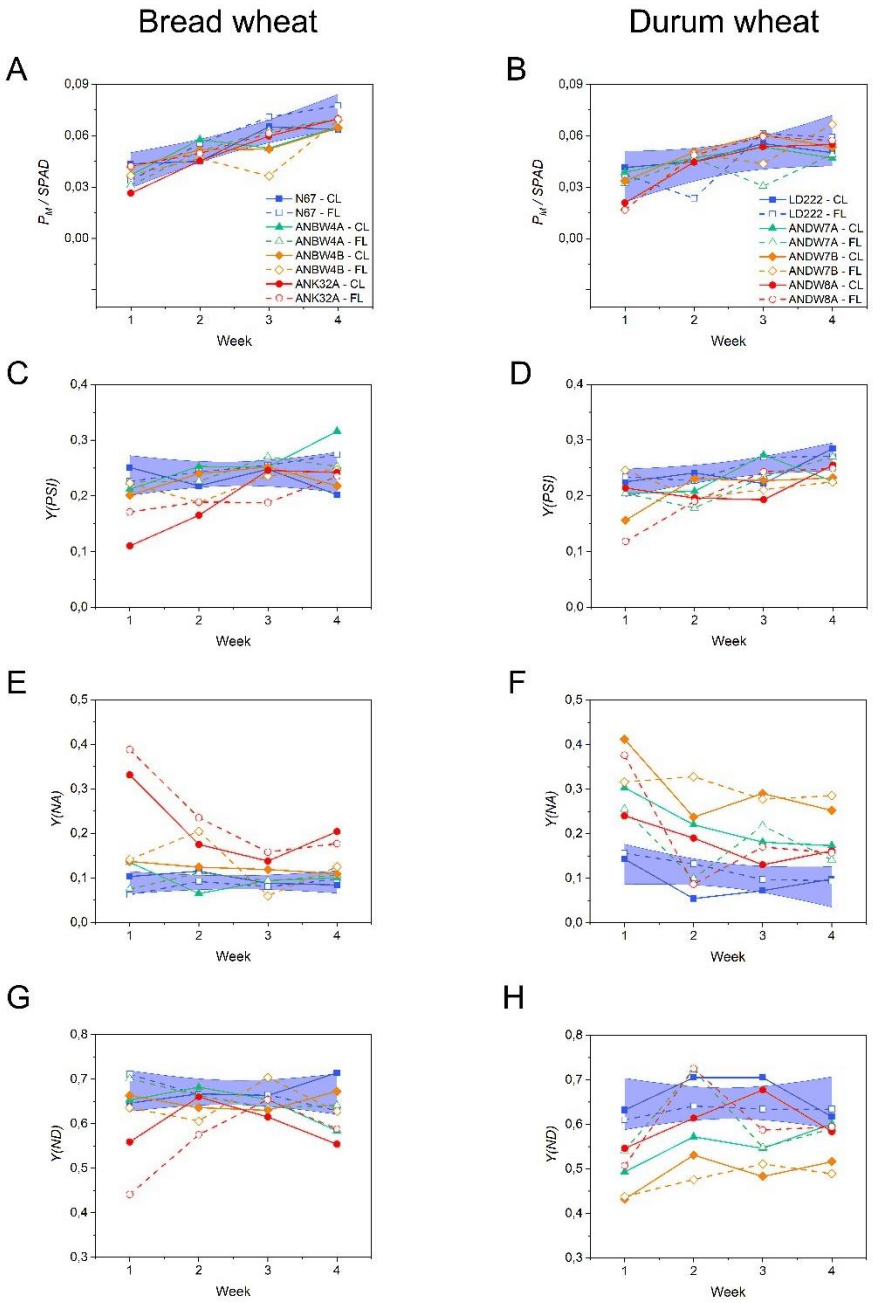

Time course of parameters related to PSI activity as emerging from Dual-PAM analyses of WT *Triticum aestivum* (bread wheat) and *T. durum* (durum wheat) and in their *chlorina* mutants, cultivated in a continuous (CL) or fluctuating light regime (FL). Photo-oxidizable PSI amount as P_M/SPAD; actual quantum of PSI photochemistry *Y(PSI)* and of non-photochemical dissipation in donor-limited PSI *Y(ND)*, or in acceptor-limited PSI *Y(NA)* were measured at the steady state in samples acclimate to high light for 7 min. Each graph reports single parameters obtained during a 4-week long monitoring, 32 to 55 DAS. For comparison of mutants, as background information in each graph the confidence bands at 95% probability are drawn after linear regression of all WT values.

Supplementary Figure 6

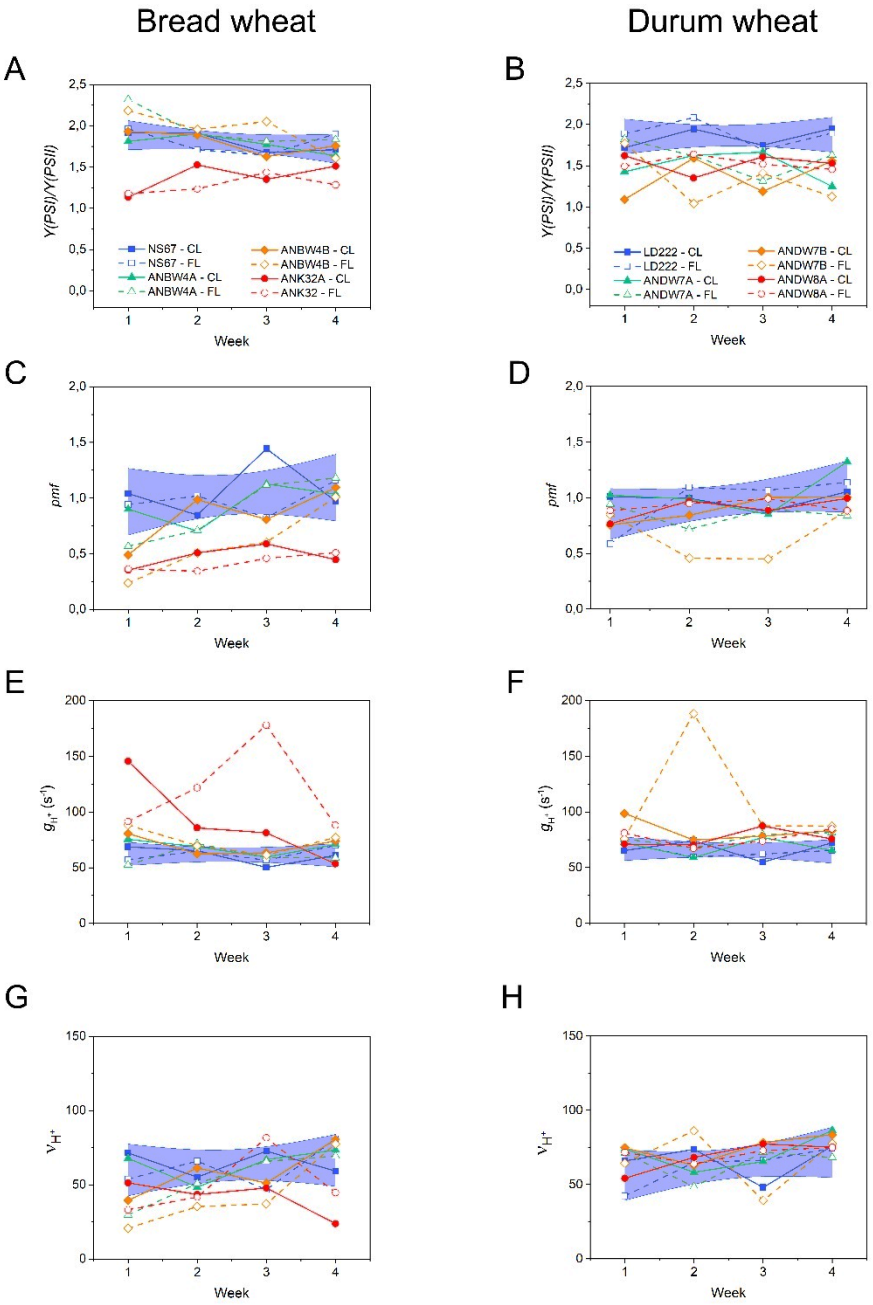

Time course of parameters related to the generation and use of the trans-thylakoidal proton motive in WT *Triticum aestivum* (bread wheat) and *T. durum* (durum wheat) and in their *chlorina* mutants, cultivated in a continuous (CL) or fluctuating light regime (FL). The quantum yield ratio *Y(PSI)/Y(PSII)* was calculated with Dual-PAM at the steady state as in Supplementary Fig. 4-5. Proton motive force *pmf*, proton conductance g_{H^+} and total proton flux v_{H^+} were calculated from the electrochromic band shift (ECS) in samples acclimated to an approximate of the growth light intensity using a JTS-100 spectrometer. Each graph reports single parameters obtained during a 4-week long monitoring, 32 to 55 DAS. For comparison of mutants, as background information in each graph the confidence bands at 95% probability are drawn after linear regression of all WT values.

Supplementary Figure 7

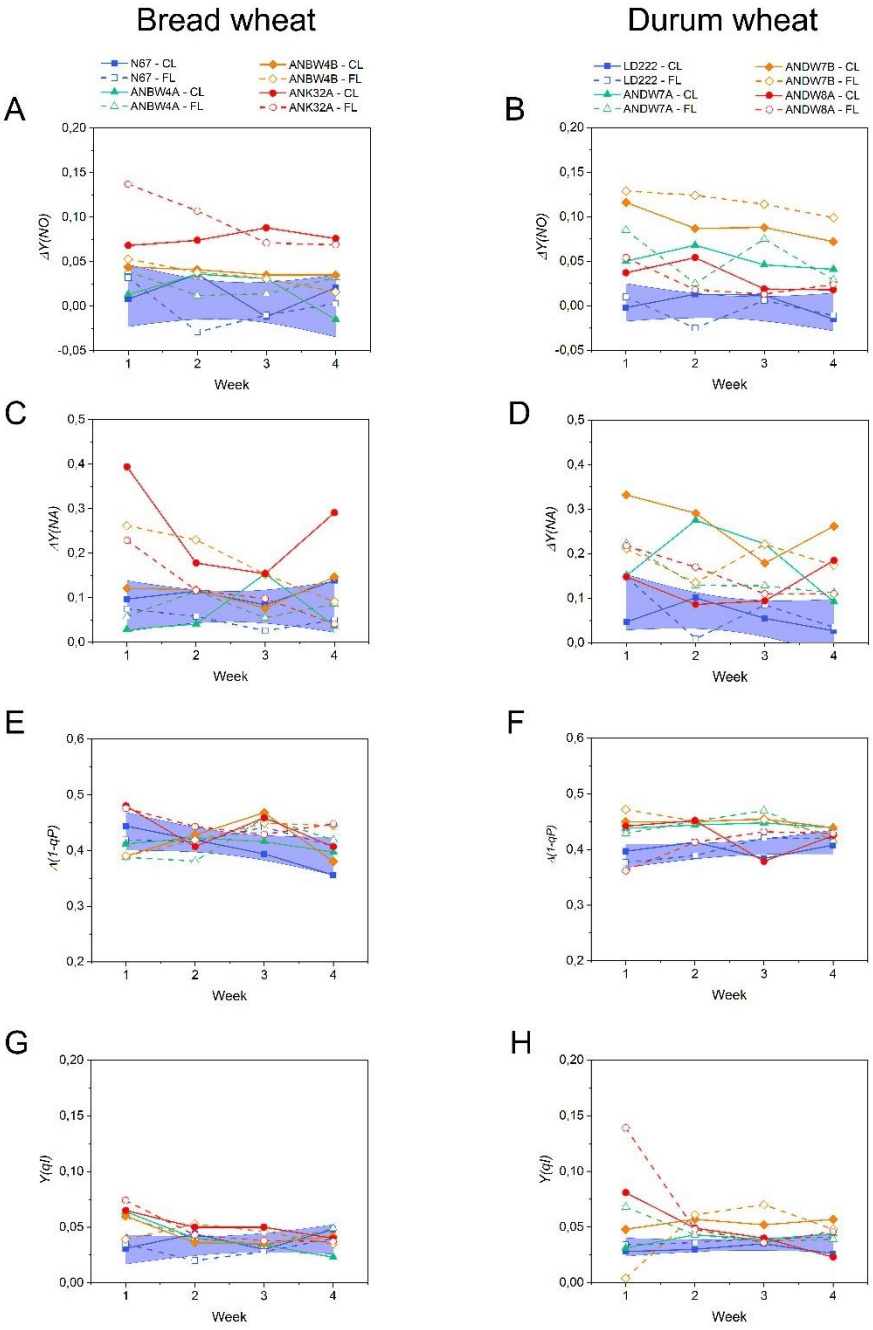

Time course of parameters related to the dynamic regulation of photosynthesis in WT *Triticum aestivum* (bread wheat) and *T. durum* (durum wheat) and in their *chlorina* mutants, cultivated in a continuous (CL) or fluctuating light regime (FL). All parameters were measured with Dual-PAM: *ΔY(NO)*, *ΔY(NA)*, *Δ(1-qP)* represent the difference in the respective parameters (defined in main text) measured during a minutes-scale rise from growth light to high light (539 to 1960 µmol photons m^{-2} s^{-1}); *Y(qI)* is PSII photoinhibition at the end of the Dual-PAM measuring routine (see Supplementary Fig. 2). Each graph reports single parameters obtained during a 4-week long monitoring, 32 to 55 DAS. For comparison of mutants, as background information in each graph the confidence bands at 95% probability are drawn after linear regression of all WT values.

Supplementary Figure 8

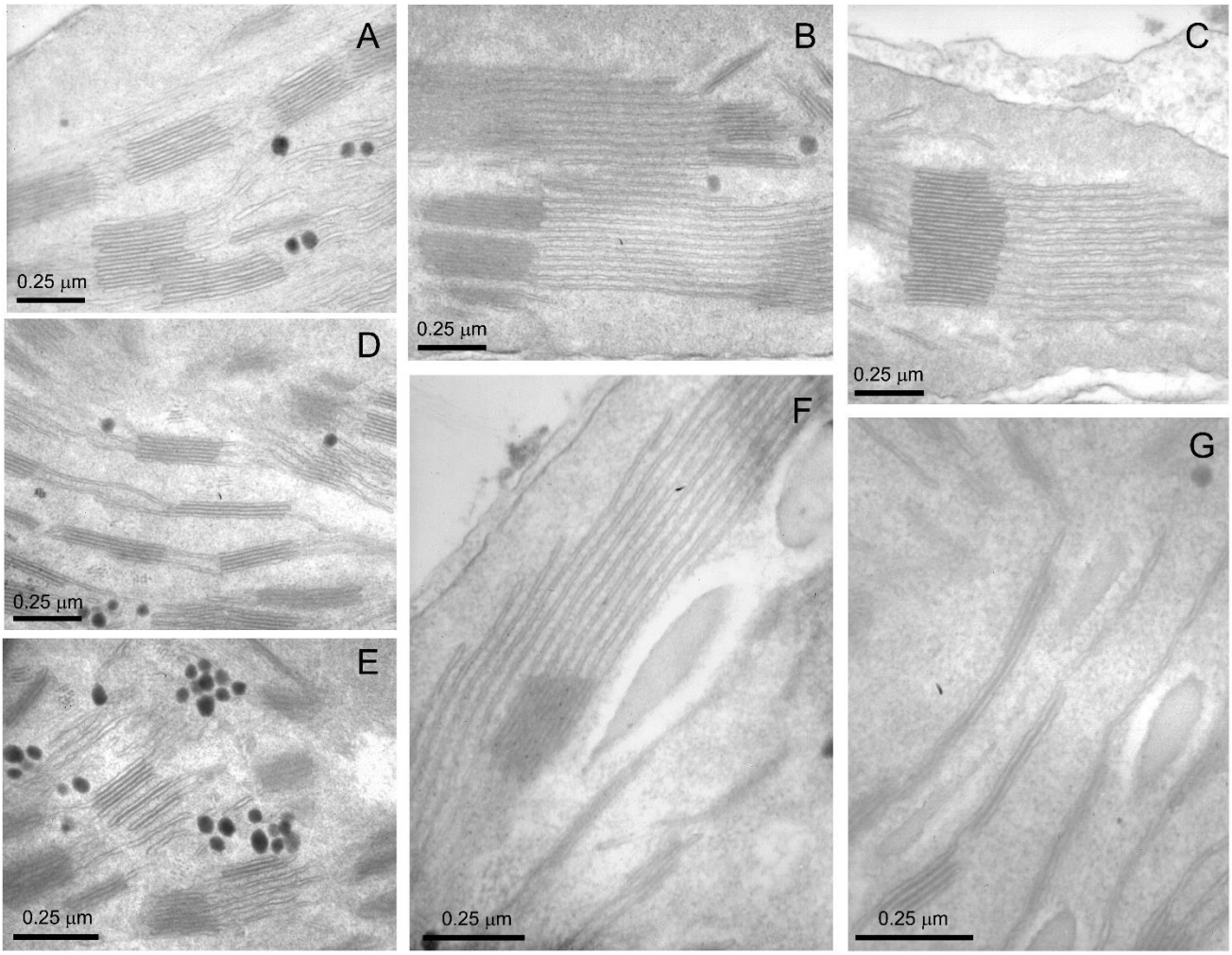

Examples of thylakoid architectures in chloroplasts of *chlorina* mutants of wheat grown under continuous (CL) or fluctuating (FL) light.

(A) Normal thylakoid system, with grana and intergrana thylakoids and few plastoglobules in LD222 grown under FL.

(B) A large array of single straight and parallel thylakoids for the example of a chloroplast in ANK32A grown under FL.

(C) An array of single straight thylakoids originating from a large granum in ANDW8A grown under CL.

(D) Small grana in ANDW8A grown under FL.

(E) Clusters of many plastoglobules associated with a disturbed thylakoid system in ANDW7A grown under FL.

(F) Arrays of single straight thylakoids co-existing with grana and short thylakoid bundles in ANDW7B grown under FL.

(G) Detail of thylakoids doublets, i.e. appressed in groups of two in ANDW7B under FL.

Supplementary Figure 9

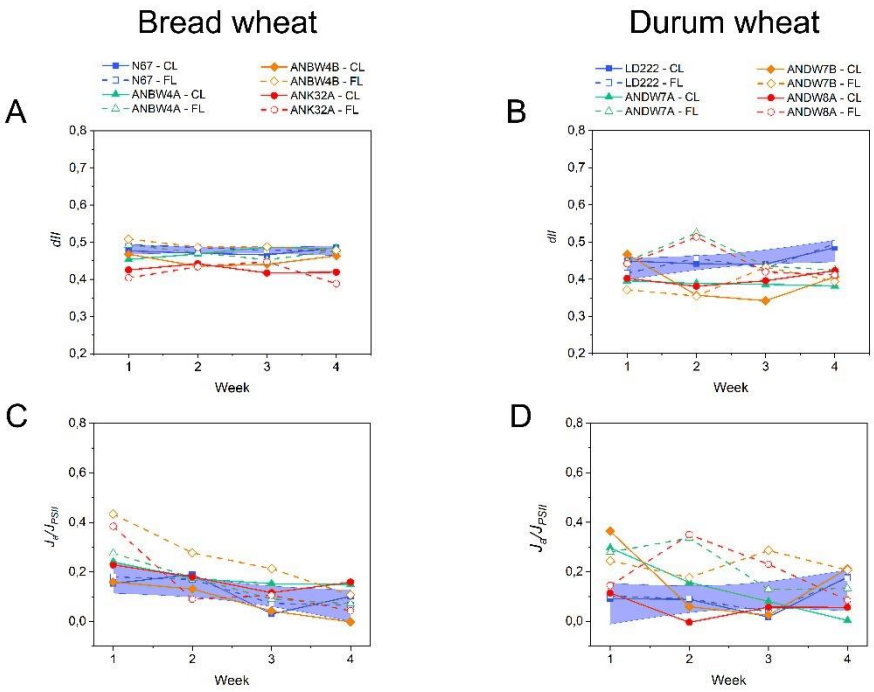

Time course of the energy distribution to PSII (*dII*) and the electron flow to electron sinks alternative to photosynthesis (J_A/J_{PSII}) in WT *Triticum aestivum* (bread wheat) and *T. durum* (durum wheat) and in their *chlorina* mutants, cultivated in a continuous (CL) or fluctuating light regime (FL).

dII was calculated from Dual-PAM parameters. J_A/J_{PSII} was calculated from simultaneous variations of chlorophyll fluorescence and CO_2 exchange. Details on calculation are in the main text.

Each graph reports single parameters obtained during a 4-week long monitoring, 32 to 55 DAS. For comparison of mutants, as background information in each graph the confidence bands at 95% probability are drawn after linear regression of all WT values.

Supplementary Figure 10

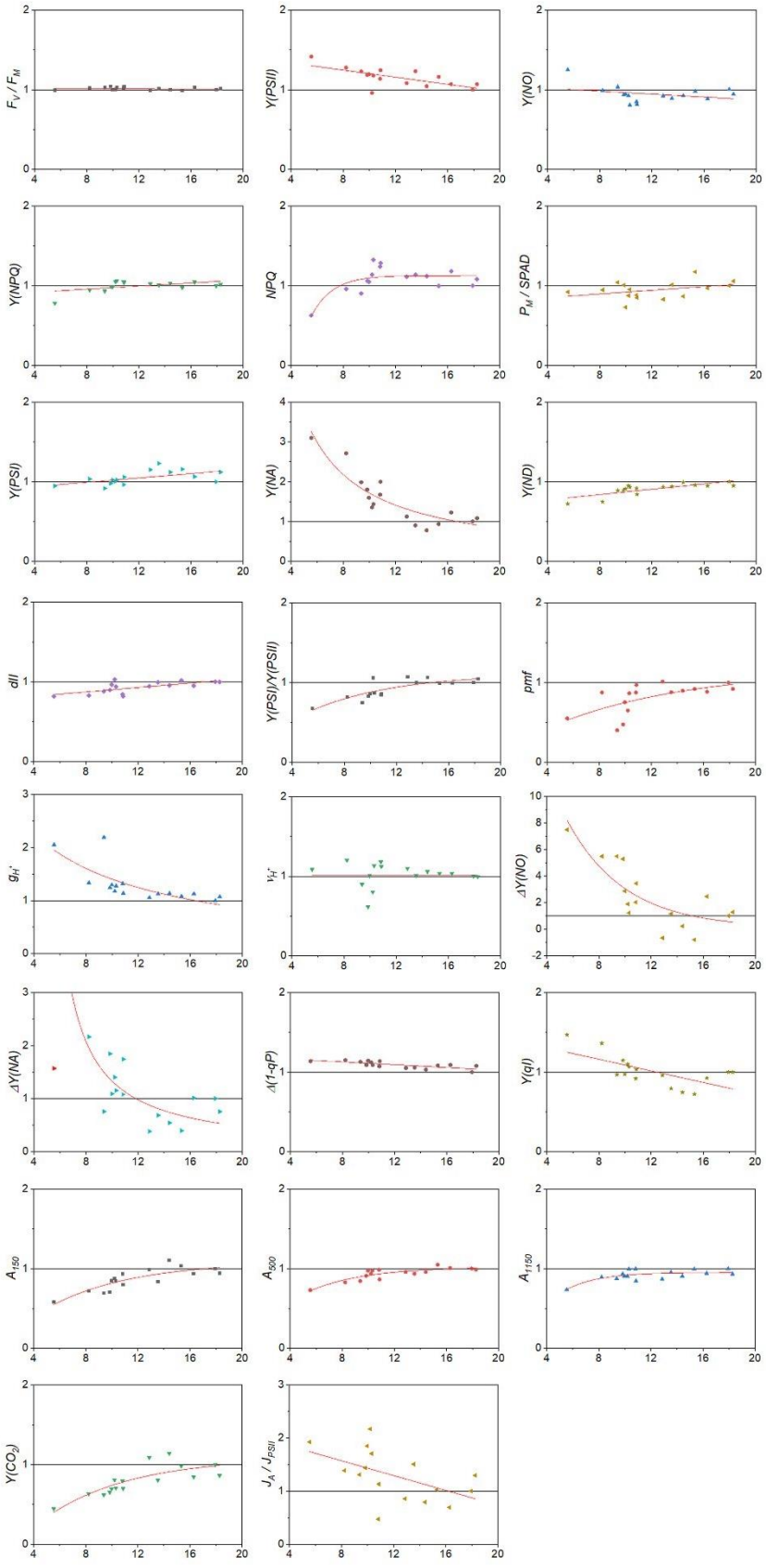

Plots of measured photosynthesis-related parameters *vs* final aboveground biomass accumulated by *Triticum* plants grown under continuous (CL) or fluctuating light (FL). For each parameter, the average values obtained over 3 or 4 weeks (see the corresponding analysis for each parameter in the main text) were normalized to the value obtained from NS67 under CL, which was therefore set to 1 for reference.

In each graph, the normalized values of each parameter were plotted against the final shoot biomass and fitted with the following functions (*y* is parameter, *x* is biomass):

- linear, $y = ax + b$
- saturating, $y = A_1 - A_2 e^{-bx}$
- reciprocal, $y = \frac{a}{1+bx}$
- exponential decay, $y = y_0 + Ae^{-\frac{x}{b}}$

The best fitting function is drawn in each graph. In all cases, all points were used for the fitting calculus, except one outlier point in the plot of *ΔY(NA)*, highlighted in red and corresponding to ANDW7B under FL.